Supporting Information

Impact of Anchoring Groups on the Photocatalytic Performance of Iridium(III) Complexes for Hydrogen Production and Their Toxicological Analysis

Xiao Yao,[a] Lin-Yu Fan, # [b] Zhu-Wu Jiang, * [a] Chao-Qun Zheng,[a] Jin-Feng Chen [a], Ya-Chen Jiang[a], Yi-Sang Lu,[a] Cheuk-Lam Ho,[b] Yuan-Mei Chen, * [c]

[a] Dr. *X. Yao, Prof. Z.W. Jiang, Dr. C.Q. Zheng, Dr. J.F. Chen, Y.C. Jiang, Y.S. Lu, X. Li, L.N. Liu*
School of Ecological Environment and Urban Construction,
Fujian University of Technology,
Fuzhou 350118, China
E-mail: Jiangzhuwu@126.com (Prof. Zhu-Wu Jiang)

[b] L.Y. Fan, Dr. C.L. Ho
Department of Applied Biology and Chemical Technology,
The Hong Kong Polytechnic University,
Hung Hom, Hong Kong (P.R. China);
PolyU Shenzhen Research Institute, Shenzhen (P. R. China).

[c] Dr. Y. M. Chen
Department of Thoracic Surgery,
School of Fujian Medical University, Fujian Cancer Hospital,
Fuzhou 350014, China
E-mail: chenym091@hotmai.com (Prof. Yuan-Mei Chen)

# These authors contributed equally to this work.

Instrumentation

Matrix-assisted laser desorption Ionization Time-of-Flight (MALDI-TOF) or Liquid Chromatography–Electrospray Ionization Quadrupole-TOF (LC-ESI-Q-TOF) mass spectrometry was performed on an Autoflex Bruker MALDI-TOF or Agilent 6540 system, respectively. ^{1}H and ^{13}C NMR spectra were measured in DMSO or $CDCl_3$ on a Bruker Ultra-shield 400 MHz FT-NMR spectroscopy and tetramethylsilane (TMS) was used as an internal standard for calibrating the chemical shift. UV/Vis absorption spectra were recorded on an Agilent Technologies Cary 8454 UV-Vis spectrometer in CH_2Cl_2 solution at 293 K. PL spectra were recorded on a Cary Eclipse Fluorescence Spectrophotometer in CH_2Cl_2 solution at 293 K. Cyclic voltammetry (CV) measurements were performed with a CHI 680D Electrochemical Analyzer/Workstation, using glassy carbon electrode as the working electrode, platinum wire as the counter electrode, and Ag/Ag^+ as the reference electrode, in acetonitrile solution containing 0.1 M tetrabutylammonium hexafluorophosphate at a scan rate of 100 mV s^{-1}. Under these conditions, the reversible oxidation potential ($E_{1/2}$) of ferrocene was 0.40 V versus Ag/Ag^+. Element mapping was performed with a TALOS F200X field emission transmission electron microscope (FEI) operating at 200 kV. Fourier-transform infrared (FT-IR) characterization were determined by Bruker Vector-22 infrared spectroscopy at room temperature. Inductively Coupled Plasma Optical Emission Spectrometery (ICP-OES) was conducted by Agilent 720ES(OES). X-Ray Diffractometer (XRD) was performed by Bruker D8 Venture.

Cyclic voltammetry measurements

Cyclic voltammetry (CV) experiments were conducted with a CHI 680D electrochemical analyser using glassy carbon as the working electrode, Pt wire as the counter electrode and Ag/Ag^+ as the reference electrode using dichloromethane comprising 0.1 M tetrabutylammonium hexafluorophosphate as the solvent at a scan rate of 100 mV s^{-1}. Under these conditions, the reversible oxidation potential ($E_{1/2}$) of ferrocene was 0.40 V versus Ag/Ag^+[1].

Electrochemical impedance spectroscopy and photocurrent measurements

Electrochemical impedance spectroscopy (EIS) was performed on an electrochemical workstation CHI660E (Shanghai Chenhua, China), using a three-electrode system comprising Ag/AgCl as the reference electrode and Pt wire as the counter electrode, with 0.5 M sodium sulphate (Na_2SO_4) solution as electrolyte. To prepare the working electrode, 10 mg of the iridium(III) dyes was dispersed in 1 mL ethanol and 20 μL Nafion aqueous solution (5 wt%) and then ultrasonically scattered for 2 h. Subsequently, 0.1 mL of the slurry was added dropwise onto an FTO glass substrate (1 cm^2). The iridium(III) dye remained coated on the FTO glass surface after the ethanol had been evaporated off. EIS was conducted in the frequency range of 0.1 Hz to 100 kHz at room temperature with the applied bias potential set at –700 mV and the alternate current amplitude set at 5 mV. Photocurrent spectra were obtained in the frequency range of 0.1 Hz to 100 kHz with an applied bias potential of –700 mV and an AC amplitude of 5 mV. Light was supplied via a 300 W Xe lamp. All the experiments were conducted at room temperature.

Preparation of platinized TiO_2

To a one-neck round bottom flask containing 1.6 g of titanium oxide powder (anatase, < 25 nm particle size, 99.7% trace metals basis, Sigma-Aldrich) and 0.1 mL of H_2PtCl_6 aqueous solution (8 wt%), 40 mL MeOH was added. The reaction mixture was then subjected to radiation by a 300 W Hg lamp (HF300PD, EYE Lighting) for 24 h with stirring. The mixture was undergone centrifugation at 4000 rpm for 5 mins and the solid obtained was washed with MeOH three times. The remaining solid was dried under vacuum in darkness overnight.

Adsorption of iridium(III) photosensitizer onto platinized TiO_2

To a centrifuge tube containing 20 mg of Pt-TiO_2, 2.5 mL of 50 μM photosensitizer in MeOH solution was added, and the mixture was then sonicated for 30 mins. The solution was decolorized and became clear gradually, while the grey color solid was changed to light pink. The tube was centrifuged at 4000 rpm for 15 mins and the liquid layer was removed by a dropper. The remaining solid was dried in darkness overnight. The whole dried pellet was directly utilized in the photocatalytic reaction. The dye-loading percentage was estimated by comparing the absorbance of the absorption peaks between the supernatant and the original photosensitizer solution (**Figure S10 - Figure S12)**.

Light-driven H_2 production studies

To a one-neck pear-shaped round bottom flask containing the dye-adsorbed platinized TiO_2, 5 mL of 0.5 M of AA (pH = 4) was added as the hole scavenger. The flask was steadily stirred and continuously radiated with 300W Xeon light (visible light, 420-800nm). The produced hydrogen was measured and quantified by GC (Agilent 6890 Series GC System with a molecular sieve 5 Å column and thermal conductivity detector).

Toxicity Testing

To investigate the toxicity of the final products generated by photocatalytic materials (**Ir1@Pt-TiO_2**, **Ir2@Pt-TiO_2**, **Ir3@Pt-TiO_2**) during the photocatalytic hydrogen production process, we assessed the toxicity of water samples containing these photocatalytic materials after a 5-hour reaction period. This evaluation was carried out in accordance with international standards (ISO11348: 2007) and the national standards of the People's Republic of China (GB/T15441-1995), utilizing Bacillus luminiformis T3 as the indicator organism[2]. The luminescent bacterium Photobacterium T3 race was employed as the test organism to quantify the biotoxicity of the photocatalytic materials' water samples both prior to and following the photocatalytic process. For detailed experimental procedures, please refer to previous research[3].

Synthesis of Materials:

2-(furan-2-yl)-5-nitropyridine: To a round bottom flask containing 2-bromo-5-nitropyridine (2.00 g, 9.85 mmol) in tetrahydrofuran (180 mL), furan-2-ylboronic acid (1.65 g, 14.78 mmol) was added. Tetrakis(triphenylphosphine)palladium(0) (1.14 g, 0.99 mmol) and 2M of potassium carbonate (30 mL, 59.11 mmol) were added to the reaction mixture, which was then heated to 85 °C for 48 h. After being cooled to room temperature, the mixture was extracted with ethyl acetate and brine. The organic layer was dried over sodium sulfate, filtered and concentrated by reduced pressure. The crude product was purified by silica gel column chromatography using dichloromethane/n-hexane (1:1, v/v) as eluent to get the final product as a yellow solid (yield: 1.62 g, 86%).^{1}H NMR (600 MHz, DMSO) δ 9.35 (dd, J = 2.7, 0.7 Hz, 1H), 8.63 (dd, J = 8.8, 2.7 Hz, 1H), 8.08 – 7.90 (m, 2H), 7.43 (dd, J = 3.5, 0.8 Hz, 1H), 6.78 (dd, J = 3.5, 1.7 Hz, 1H). ^{13}C NMR (151 MHz, DMSO) δ 153.05, 152.05, 147.26, 145.88, 142.69, 133.33, 118.69, 113.94, 113.75. Found: $[M+H]^+$ 191.0454; 'molecular formula $C_9H_6N_2O_3$ ' requires $[M+H]^+$ 191.0451.

2-(5-bromofuran-2-yl)-5-nitropyridine: To a round bottom flask containing 2-(furan-2-yl)-5-nitropyridine (1.00 g, 5.26 mmol) in dichloromethane (10 mL), N-bromosuccinimide (1.12 g, 6.31 mmol) was added slowly. The reaction mixture was stirred at room temperature overnight. After the reaction finished, 20 mL DI water was added into the mixture slowly resulting in many yellow precipitates that collected by filtration. The crude product was purified by silica gel column chromatography using n-hexane as eluent to give the target product as a yellow solid (1.29 g, 91%). ^{1}H NMR

(600 MHz, DMSO) δ 9.39 – 9.21 (m, 1H), 8.63 (ddd, *J* = 8.8, 2.7, 0.8 Hz, 1H), 8.14 – 7.80 (m, 1H), 7.47 (dd, *J* = 3.6, 0.9 Hz, 1H), 6.91 (dd, *J* = 3.6, 0.8 Hz, 1H). ^{13}C NMR (151 MHz, DMSO) δ 153.84, 151.81, 145.89, 142.88, 133.42, 126.72, 118.81, 116.27, 115.86. Found: $[M+H]^+$ 268.9558; 'molecular formula $C_9H_5N_2BrO_3$ ' requires $[M+H]^+$ 268.9556.

4-(5-(5-nitropyridin-2-yl)furan-2-yl)-N,N-diphenylaniline: To a round bottom flask containing 2-(5-bromofuran-2-yl)-5-nitropyridine (1.00 g, 3.72 mmol) in tetrahydrofuran (180 mL), (4-(diphenylamino)phenyl)boronic acid (1.61 g, 5.58 mmol) was added. Tetrakis(triphenylphosphine)palladium(0) (0.43 g, 0.37 mmol) and 2M of potassium carbonate (12 mL, 22.30 mmol) were added to the reaction mixture, which was then heated to 85 °C for 48 h. After being cooled to room temperature, the mixture was extracted with ethyl acetate and brine. The organic layer was dried over sodium sulfate, filtered and concentrated by reduced pressure. The crude product was purified by silica gel column chromatography using dichloromethane/n-hexane (1:1, v/v) as eluent to get the final product as a red solid (1.37 g, 85%).^{1}H NMR (400 MHz, DMSO) δ 9.38 (d, *J* = 2.6 Hz, 2H), 8.64 (dd, *J* = 8.9, 2.7 Hz, 2H), 8.07 (d, *J* = 8.9 Hz, 2H), 7.82 (d, *J* = 8.8 Hz, 2H), 7.55 (d, *J* = 3.7 Hz, 1H), 7.42 – 7.23 (m, 3H), 7.20 – 6.90 (m, 7H). ^{13}C NMR (151 MHz, DMSO) δ 156.98, 152.81, 150.98, 148.26, 147.09, 146.07, 142.26, 133.19, 130.21, 126.13, 125.14, 124.31, 123.30, 122.70, 118.46, 116.76, 108.63. Found: $[M+H]^+$ 434.1497; 'molecular formula $C_{27}H_{19}N_3O_3$ ' requires $[M+H]^+$ 434.1499.

Ir1: To a round bottom flask containing **L1** (1.00 g, 2.31 mmol), iridium(III) chloride hydrate (0.27 g, 0.77 mmol) was added with 2-ethoxyethanol: deionized water (3:1, v/v, total 8 mL). The reaction mixture was heated at 90 °C for 20 h. The reagent was purified by filtration to give the yellow solid as the iridium dimer **$Ir_2L1_4Cl_2$**. This compound was used in the subsequent reaction without further purification.

To a round bottom flask containing iridium dimer **$Ir_2L1_4Cl_2$**(0.40 g, 0.18 mmol) in dichloromethane: methanol (1:1, v/v, total 6 mL), tetraethyl [2,2'-Bipyridine]-4,4'-diylbis(phosphonate) (0.19 g, 0.46 mmol) was added. The reaction mixture was then heated to 65 °C for 6 h. After cooling to room temperature, the pH was adjusted to 5 by introducing an appropriate amount of 1M HCl. The precipitate was filtered. The crude product was purified by silica gel column chromatography using dichloromethane/methanol (1:1, v/v) as eluent to get the final product as a yellow solid (yield: 0.085 g, 31%). ^1H NMR (600 MHz, CD_2Cl_2) δ 8.78 8– 8.70 (m, 1H), 8.70 – 8.61 (m, 1H), 7.82 – 7.68 (m, 3H), 7.67 – 7.55 (m, 3H), 7.52 (d, J = 8.2 Hz, 1H), 7.47 – 7.36 (m, 2H), 7.30 – 7.15 (m, 11H), 7.14 – 6.91 (m, 20H), 4.27 – 4.01 (m, 8H), 1.37 – 1.21 (m, 12H). Found: $[M]^+$ 1485.3611; 'molecular formula $C_{72}H_{62}IrN_8O_{12}P_2$ ' requires $[M]^+$ 1485.3593

Ir2: To a round bottom flask containing iridium dimer **$Ir_2L1_4Cl_2$**(0.20 g, 0.09 mmol) in dichloromethane: methanol (1:1, v/v, total 6 mL), [2,2'-Bipyridine]-4,4'-dicarboxylic acid (0.06 g, 0.23 mmol) was added. The reaction mixture was then heated to 65 °C for

6 h. After cooling to room temperature, the pH was adjusted to 5 by introducing an appropriate amount of 1M HCl. The precipitate was filtered. The crude product was purified by silica gel column chromatography using dichloro-methane/methanol (1:1, v/v) as eluent to get the final product as a yellow solid (yield: 0.05 g, 39%).^{1}H NMR (600 MHz, CD_2Cl_2) δ 8.40 (dd, *J* = 8.8, 2.6 Hz, 2H), 7.79 (d, *J* = 8.8 Hz, 2H), 7.59 (d, *J* = 8.7 Hz, 2H), 7.27 – 7.14 (m, 10H), 7.14 – 6.78 (m, 28H). Found: $[M]^+$ 1301.2820; 'molecular formula $C_{66}H_{44}IrN_8O_{10}$ ' requires $[M]^+$ 1301.2810

Ir3: To a round bottom flask containing iridium dimer **$Ir_2L1_4Cl_2$**(0.20 g, 0.09 mmol) in dichloromethane: methanol (1:1, v/v, total 6 mL), 4,4-dinitro-2,2-Bipyridine (0.06 g, 0.23 mmol) was added. The reaction mixture was then heated to 65 °C for 6 h. After cooling to room temperature, the pH was adjusted to 5 by introducing an appropriate amount of 1M HCl. The precipitate was filtered. The crude product was purified by silica gel column chromatography using dichloro-methane/methanol (1:1, v/v) as eluent to get the final product as a yellow solid (yield: 0.04 g, 33%).^{1}H NMR (600 MHz, CD_2Cl_2) δ 8.40 (dd, *J* = 8.8, 2.6 Hz, 1H), 8.04 (dt, *J* = 5.7, 2.9 Hz, 1H), 7.79 (d, *J* = 8.8 Hz, 1H), 7.59 (d, *J* = 8.7 Hz, 2H), 7.54 – 7.47 (m, 2H), 7.30 – 7.15 (m, 12H), 7.15 – 6.92 (m, 23H). Found: $[M]^+$ 13303.3448; 'molecular formula $C_{64}H_{42}IrN_{10}O_{10}$ ' requires $[M]^+$ 1303.2714.

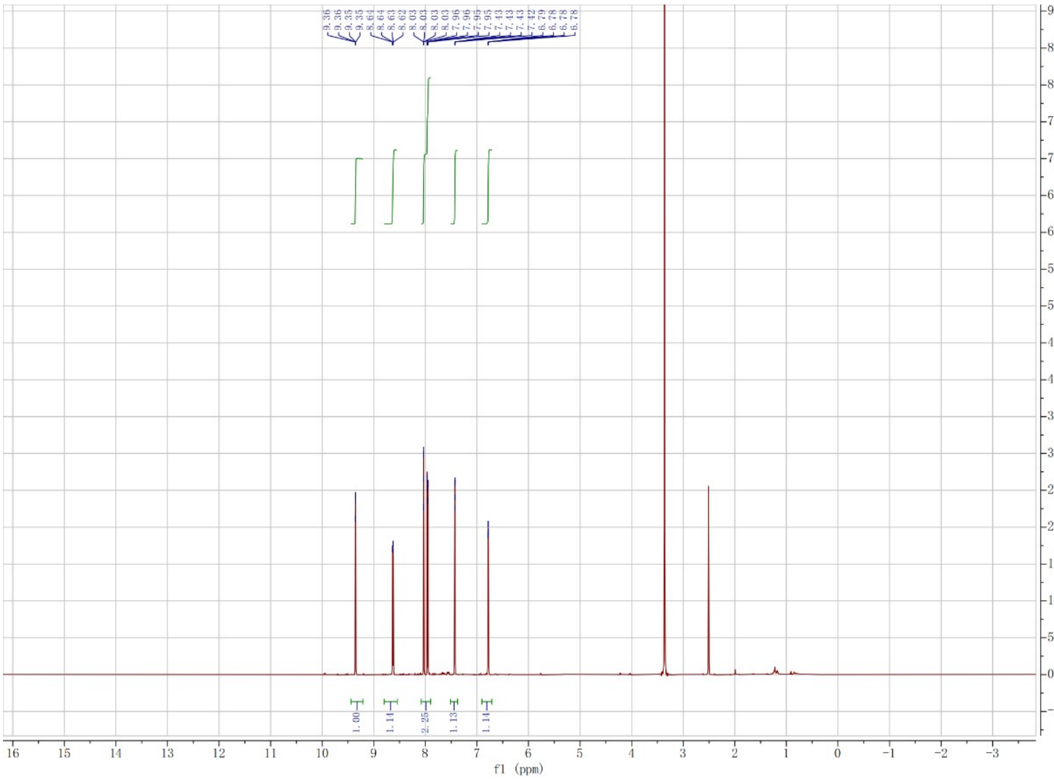

Figure S1: ^{1}H NMR spectrum of **2-(furan-2-yl)-5-nitropyridine** in DMSO-d6.

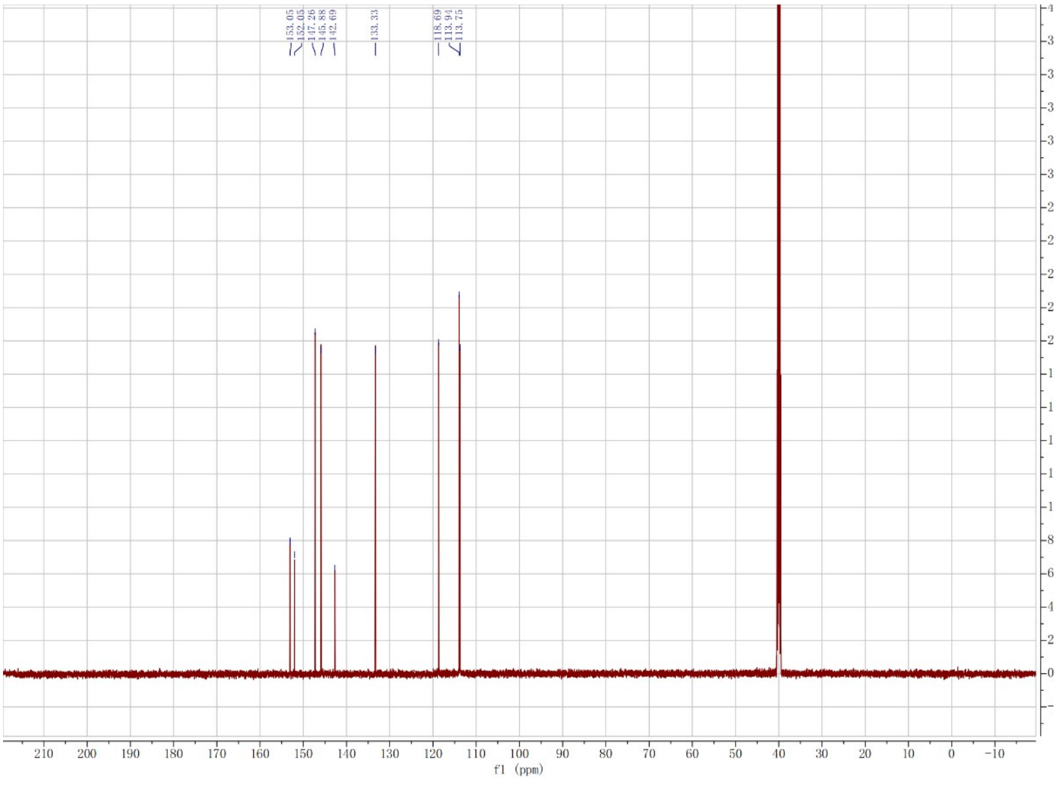

Figure S2: ^{13}C NMR spectrum of **2-(furan-2-yl)-5-nitropyridine** in DMSO-d6.

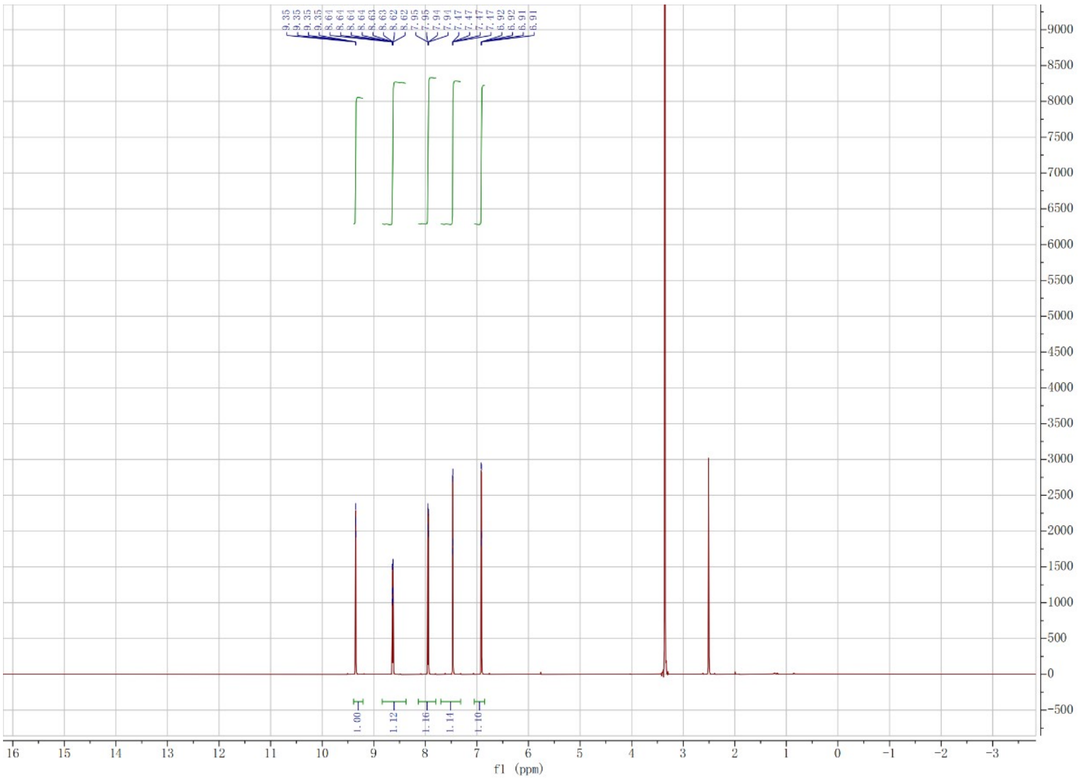

Figure S3: ^{1}H NMR spectrum of **2-(5-bromofuran-2-yl)-5-nitropyridine** in DMSO-d6.

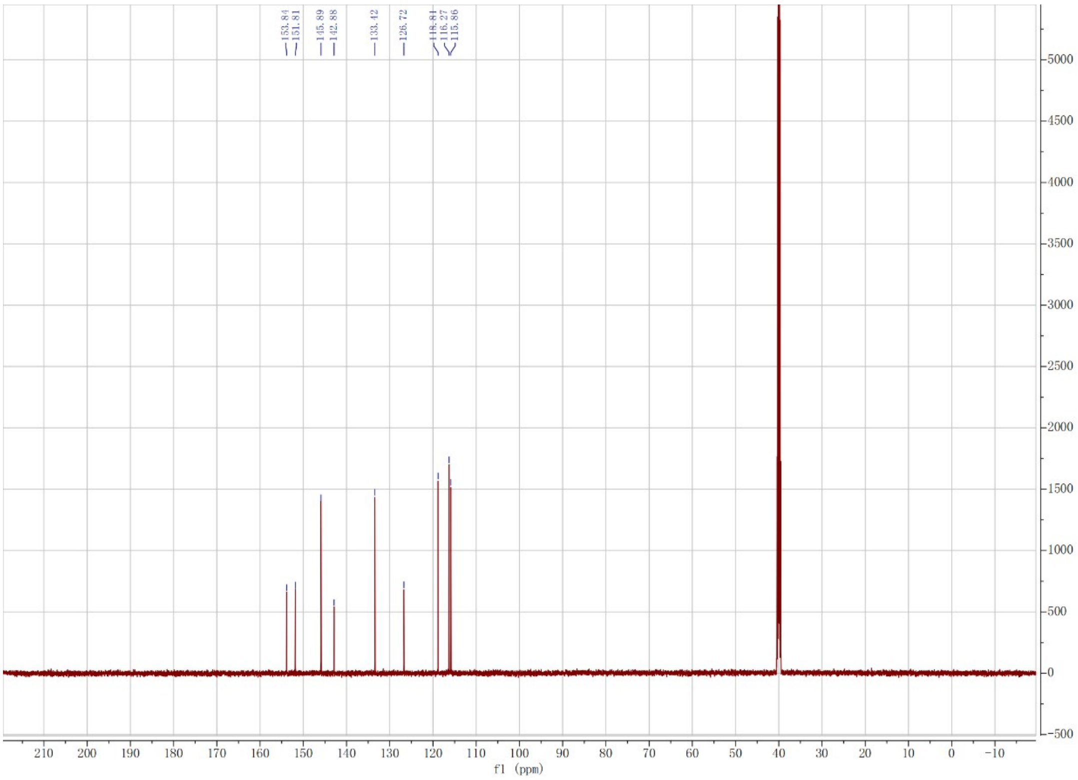

Figure S4: ^{13}C NMR spectrum of **2-(5-bromofuran-2-yl)-5-nitropyridine** in DMSO-d6.

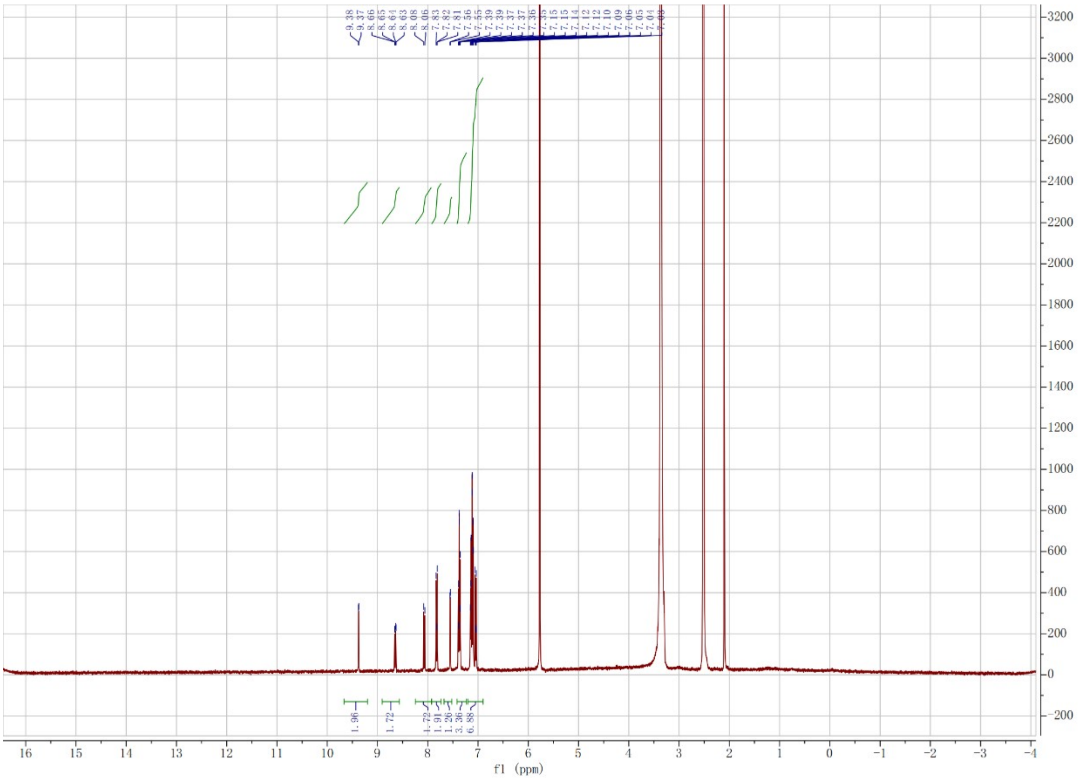

Figure S5: ^{1}H NMR spectrum of **L1** in DMSO-d6.

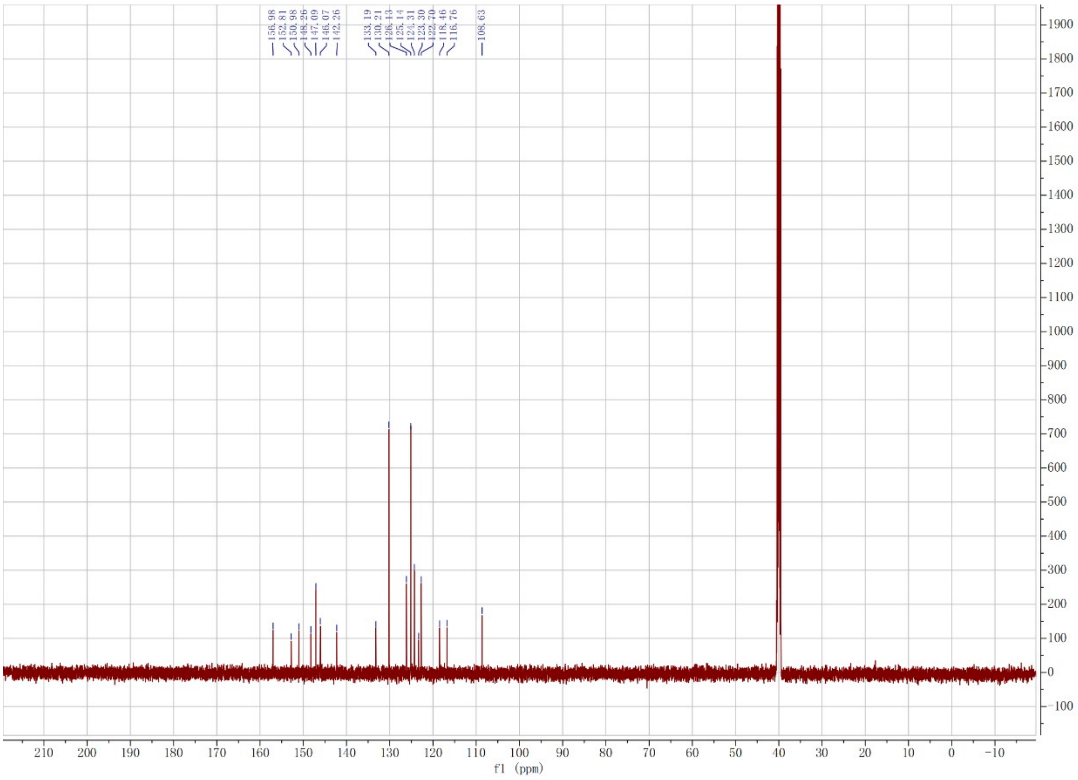

Figure S6: ^{13}C NMR spectrum of **L1** in DMSO-d6.

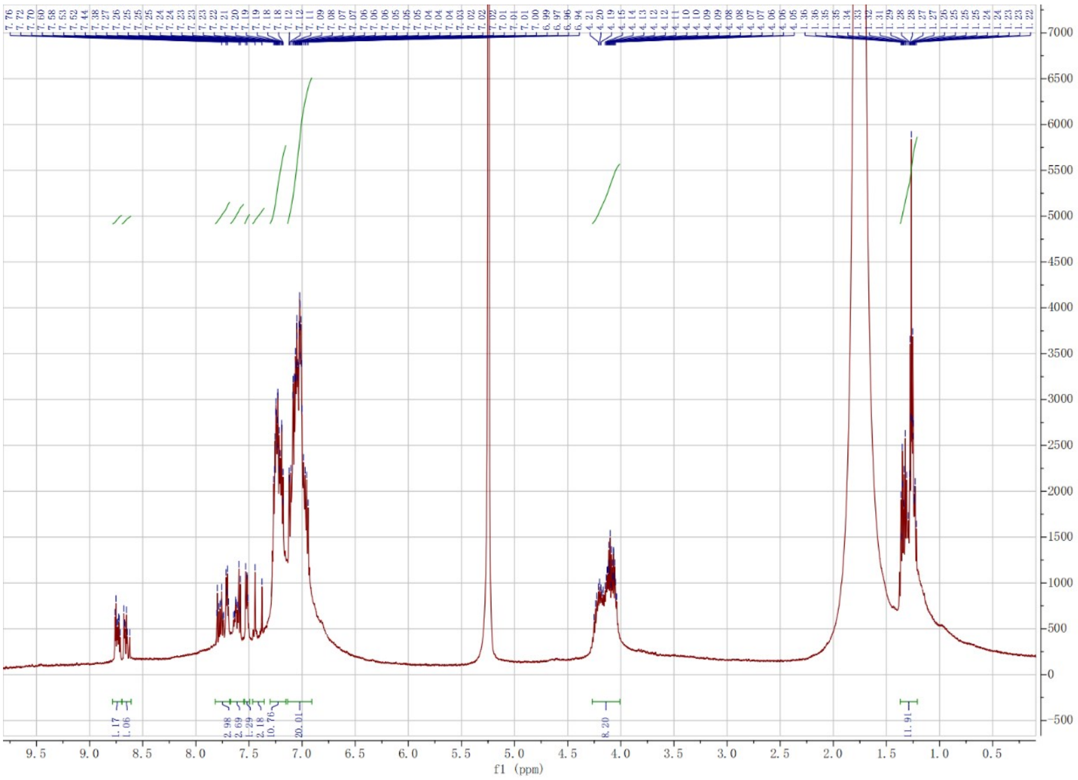

Figure S7: ^{1}H NMR spectrum of **Ir1** in CD_2Cl_2

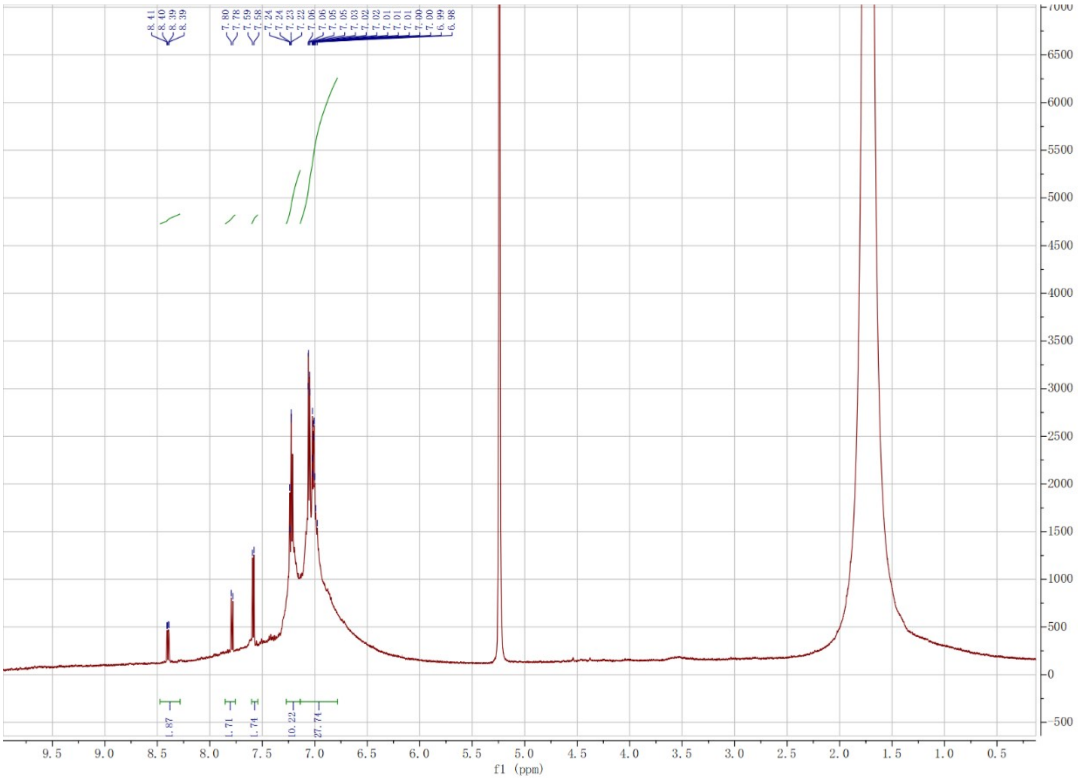

Figure S8: ^{1}H NMR spectrum of **Ir2** in CD_2Cl_2

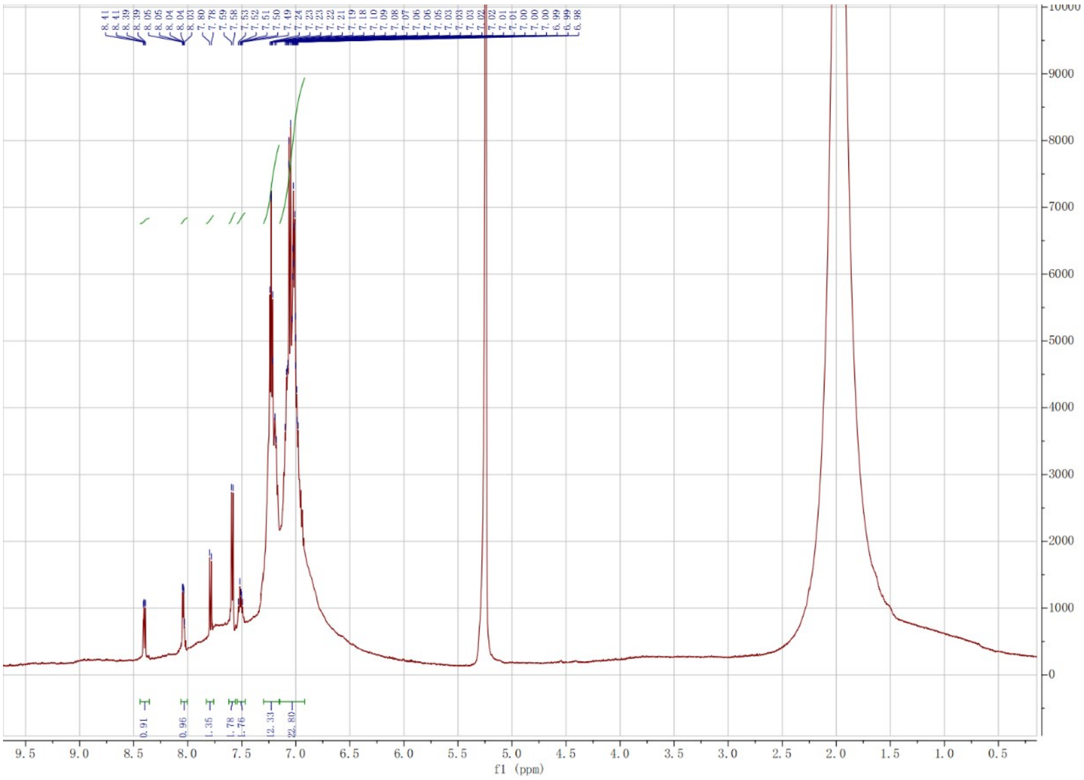

Figure S9: ^{1}H NMR spectrum of **Ir3** in CD_2Cl_2

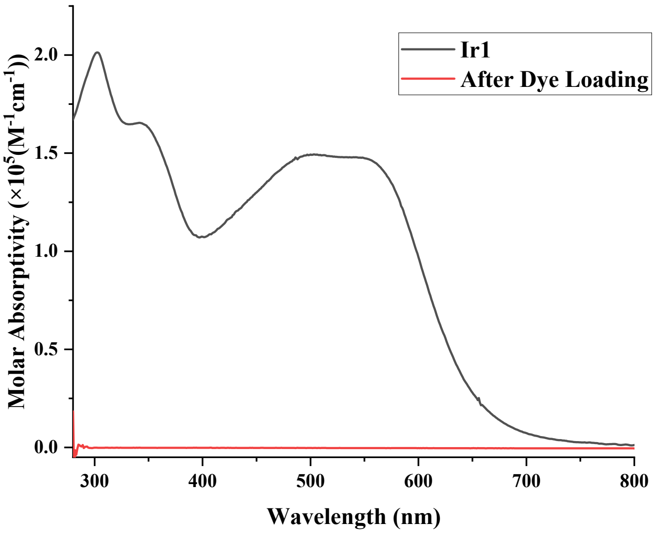

Figure S10: UV/Vis absorption spectra of **Ir1** before and after dye loading in CH_2Cl_2 solution at 293 K.

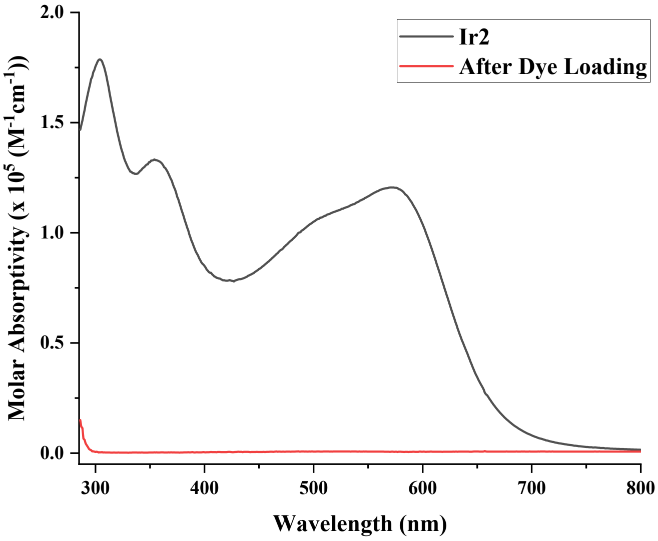

Figure S11: UV/Vis absorption spectra of **Ir2** before and after dye loading in CH_2Cl_2 solution at 293 K.

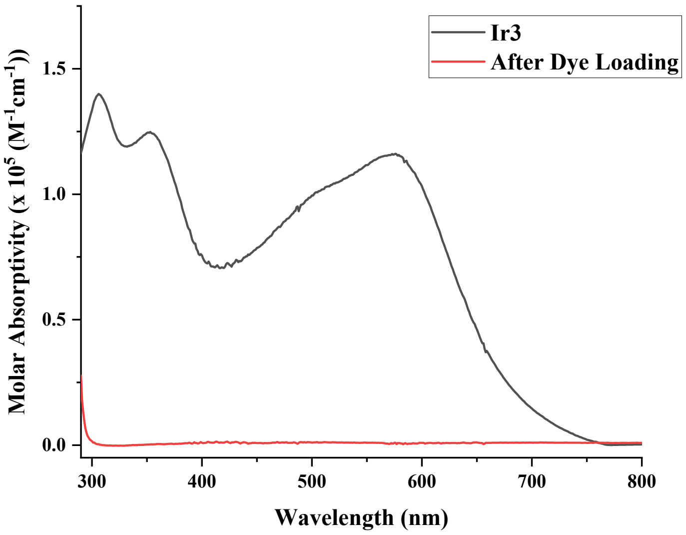

Figure S12: UV/Vis absorption spectra of **Ir3** before and after dye loading in CH_2Cl_2 solution at 293 K.

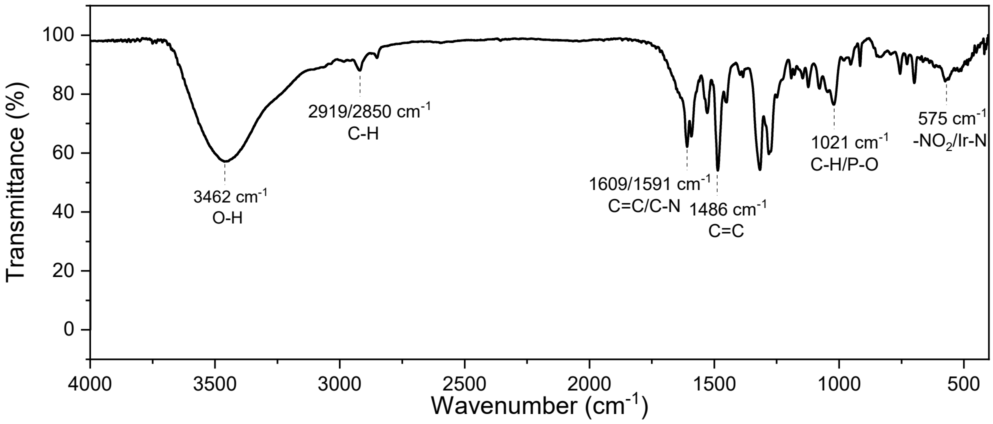

Figure S13: FTIR spectrum of **Ir1**

Table S1. FTIR spectral analysis of **Ir1**

Band (cm^{-1})	**Stretching Vibration Assignment**	**Reference**
3462	-OH	[4]
2919/2850	C-H	[5-7]

1609	C=C/C=N	[5,6,8]
1591	C=C/C-N	[5,6]
1528	C=C	[5,6]
1486	C=C/C-N	[7,9,10]
1451	C=C	[5,6]
1317/1282	C=C/P=O/C-O	[5,6,11]
1021	C-H/C-O/P-O	[4,10-12]
756	C-H	[4,10]
699	C-H	[4,10]
575	-NO_2/Ir-N	[13,14]

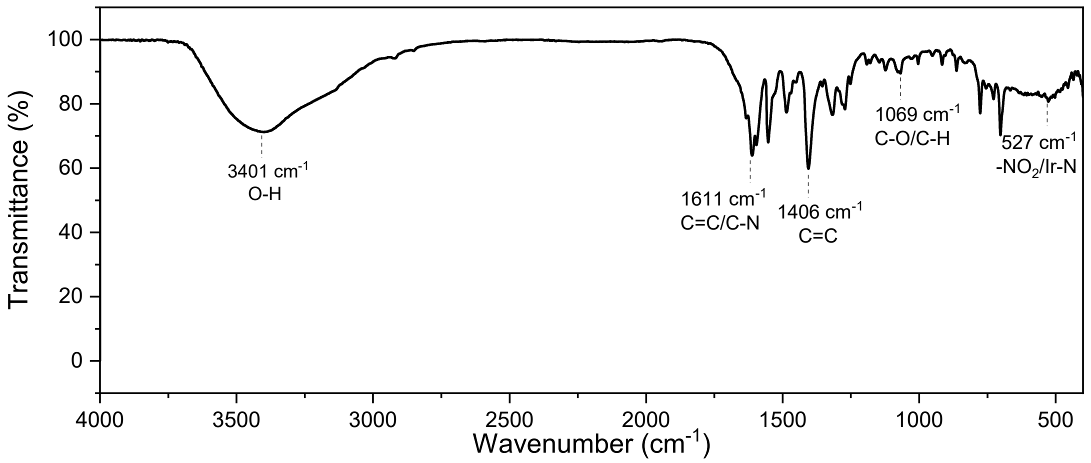

Figure S14: FTIR spectrum of **Ir2**

Table S2. FTIR spectral analysis of **Ir2**

Band (cm^{-1})	**Stretching Vibration Assignment**	**Reference**
3401	-OH	[4]
1632	C=C/C=N/C=O	[5,6,8]
1611	C=C	[5,6,8]
1596	C=C/C-N	[5,6]
1486	C=C/C-N	[7,9,10]
1406	C=C	[5,6]
1317/1272	C=C/C-O	[5,6,13]
1069	C-H/C-O	[4,10,12]
777	C-H	[4,10]

702	C-H	[4,10]
527	$-NO_2$/Ir-N	[13,14]

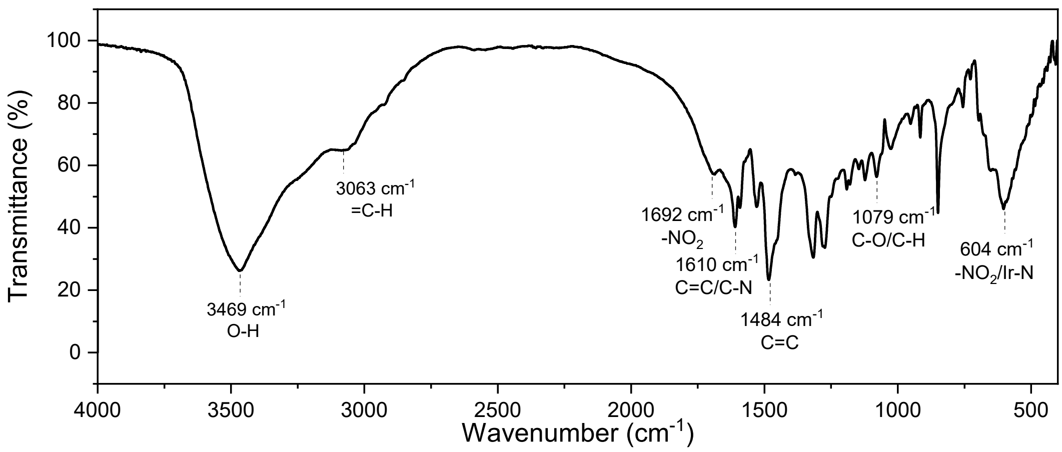

Figure S15: FTIR spectrum of **Ir3**

Table S3. FTIR spectral analysis of **Ir3**

Band (cm^{-1})	**Stretching Vibration Assignment**	**Reference**
3469	-OH	[4]
3063	=C-H	[5-7]
1692	$-NO_2$	[14]
1610	C=C/C=N	[5,6,8]
1529	C=C/C-N	[5,6]
1484	C=C/C-N	[7,9,10]
1317/1274	C=C/C-O	[5,6,13]
1079	C-H/C-O	[4,10,12]
849	C-H	[4,10]
756	C-H	[4,10]
604	$-NO_2$/Ir-N	[13,14]

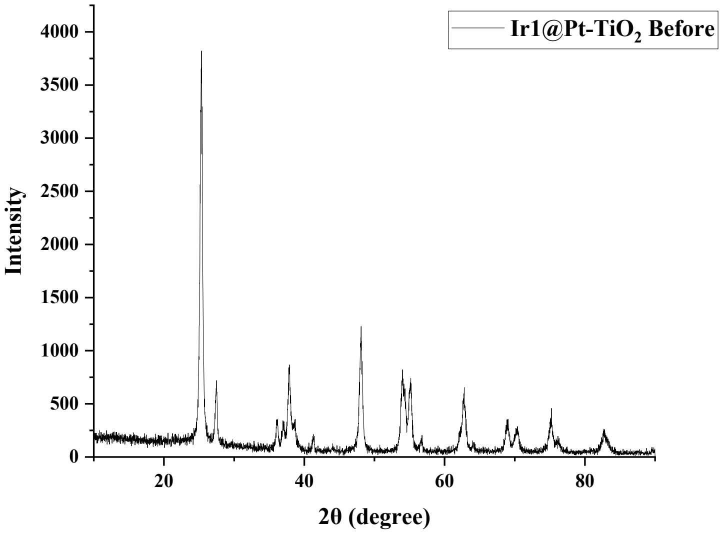

Figure S16. XRD of **Ir1@Pt–TiO$_2$** (before water-splitting experiments)

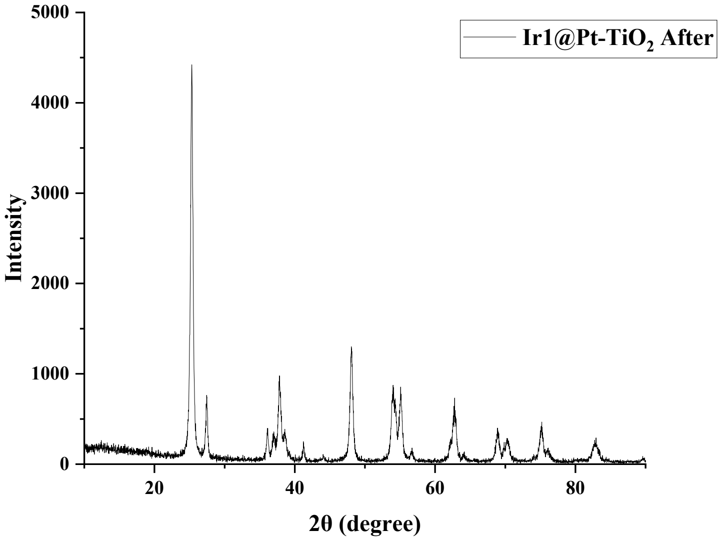

Figure S17. XRD of **Ir1@Pt–TiO$_2$** (after water-splitting experiments)

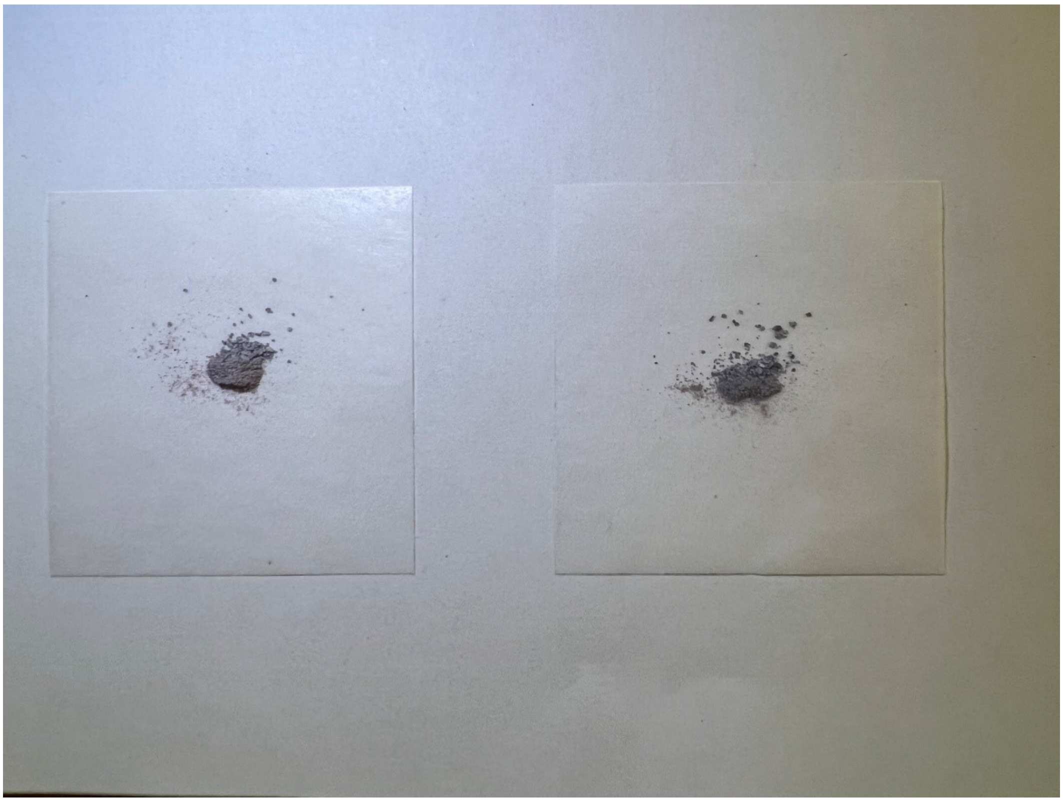

Figure S18. Ir1@Pt–TiO$_2$ before (left) and after (right) irradiation.

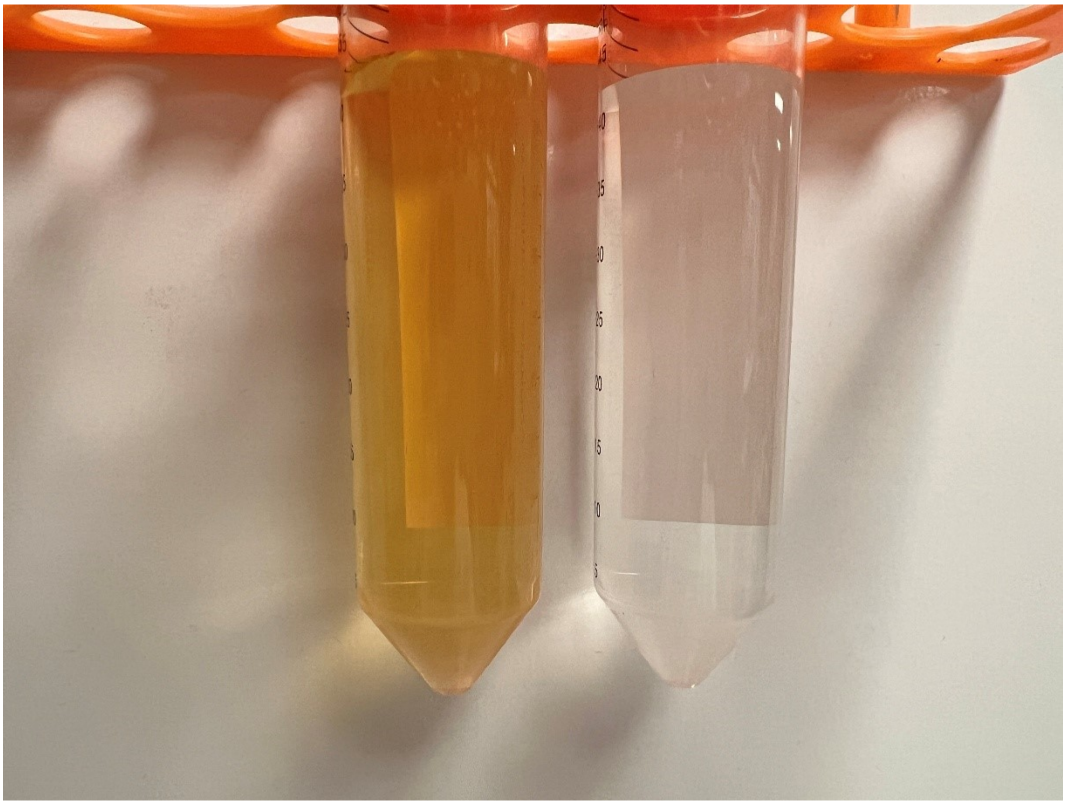

Figure S19. AA aqueous solution before (right) and after (left) irradiation.

Table S4. ICP-OES analysis result of the intensity for before and after Pt loading

	Test Element	**Test Solution Element Concentration (mg/L)**	**Digestate/Original Sample Solution Element Concentration (mg/L)**	**Sample Element Content (μg/L)**
1	Pt	<0.02	<0.02	/
2	Pt	<0.02	<0.02	/
3	Pt	<0.02	<0.02	/

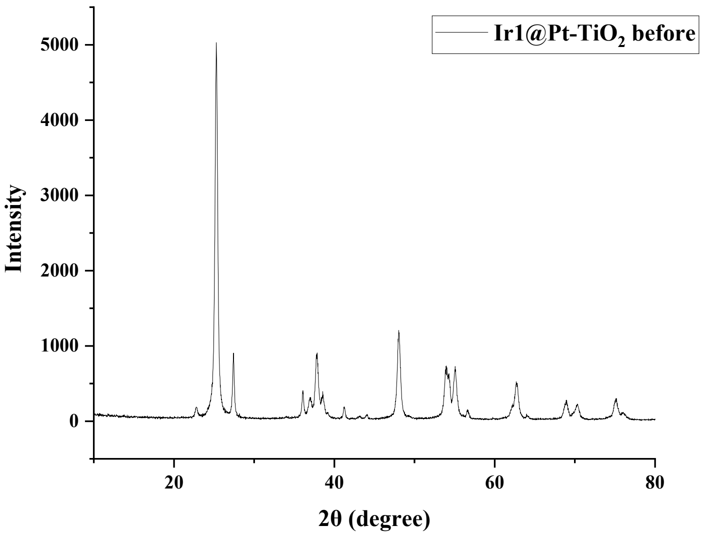

Figure S20. XRD of **Pt–TiO$_2$**

1. Baglio, J.A.; Calabrese, G.S.; Harrison, D.J.; Kamieniecki, E.; Ricco, A.J.; Wrighton, M.S.; Zoski, G.D. Electrochemical characterization of p-type semiconducting tungsten disulfide photocathodes: efficient photoreduction processes at semiconductor/liquid electrolyte interfaces. *J. Am. Chem. Soc.* **1983**, *105*, 2246–2256. https://doi.org/10.1021/ja00346a024
2. Hong, G.; Antaris, A.L.; Dai, H. Near-infrared fluorophores for biomedical imaging. *Nature biomedical engineering* **2017**, *1*, 0010.
3. Yao, X.; Fan, L.; Zhang, Q.; Zheng, C.; Yang, X.; Lu, Y.; Jiang, Y. Impact of Anchoring Groups on the Photocatalytic Performance of Iridium (III) Complexes and Their Toxicological Analysis. *Molecules* **2024**, *29*, 2564.
4. Dahule, H.; Dhoble, S.; Ahn, J.-S.; Pode, R. Synthesis and photophysics of a new deep red soluble phosphorescent iridium (III) complex based on chlorine-methyl-substituted 2, 4 diphenyl quinoline. *Journal of Physics and Chemistry of Solids* **2011**, *72*, 1524-1528.
5. Wang, Y.; Zhang, W.; Wu, X.; Luo, C.; Wang, Q.; Li, J.; Hu, L. Conducting polymer coated metal-organic framework nanoparticles: facile synthesis and enhanced electromagnetic absorption properties. *Synthetic Metals* **2017**, *228*, 18-24.
6. Liu, P.; Huang, Y.; Zhang, X. Cubic NiFe2O4 particles on graphene–polyaniline and their enhanced microwave absorption properties. *Composites Science and Technology* **2015**, *107*, 54-60.
7. Alizadeh, N.; Salimi, A.; Hallaj, R.; Fathi, F.; Soleimani, F. Ni-hemin metal–organic framework with highly efficient peroxidase catalytic activity: toward colorimetric cancer cell detection and targeted therapeutics. *Journal of nanobiotechnology* **2018**, *16*, 1-14.
8. Ge, W.J.; Shao, Q.; Xu, H.; Wan, Y.L. Low Temperature Oxidation Effects on Lignite Molecular Structure. *Advanced Materials Research* **2012**, *550*, 2797-2800.
9. Chen, R.; Zhao, G.; Yang, X.; Jiang, X.; Liu, J.; Tian, H.; Gao, Y.; Liu, X.; Han, K.; Sun, M. Photoinduced intramolecular charge-transfer state in thiophene-π-conjugated donor–acceptor molecules. *Journal of Molecular Structure* **2008**, *876*, 102-109.
10. Ehrendorfer, C.; Neugebauer, H.; Neckel, A.; Bäuerle, P. An FTIR spectroscopic study on end-capped oligothiophenes as model compounds for polythiophene. *Synthetic metals* **1993**, *55*, 493-498.
11. Shih, P.; Yung, S.; Chin, T. FTIR and XPS studies of P2O5–Na2O–CuO glasses. *Journal of Non-Crystalline Solids* **1999**, *244*, 211-222.
12. Hafeez, M.; Afyaz, S.; Khalid, A.; Ahmad, P.; Khandaker, M.U.; Sahibzada, M.U.K.; Ahmad, I.; Khan, J.; Alhumaydhi, F.A.; Emran, T.B. Synthesis of cobalt and sulphur doped titanium dioxide photocatalysts for environmental applications. *Journal of King Saud University-Science* **2022**, *34*, 102028.

13. Duan, J.; Sontarp, E.J.; Myneni, S.C. Detecting Structural Environments of Carboxyl Groups in Dissolved Natural Organic Molecules. *ACS ES&T Water* **2024**, *4*, 555-563.
14. Sangeetha, M.; Mathammal, R. A complete synergy on the experimental and theoretical study of the pyridine derivatives–2-Hydroxy-5-Nitropyridine and 2-Chloro-5-Nitropyridine. *Journal of Molecular Structure* **2016**, *1117*, 121-134.